ISSN 1070-3632, Russian Journal of General Chemistry, 2013, Vol. 83, No. 8, pp. 1493–1500. © Pleiades Publishing, Ltd., 2013.
Original Russian Text © A.I. Ermakov, I.V. Yurova, A.D. Davydov, B.A. Khorishko, A.P. Lar'kov, K.V. Stanislavchik, 2013, published in Zhurnal Obshchei Khimii, 2013, Vol. 83, No. 8, pp. 1258–1266.

The Structure of Minimal Magnetite Cluster

A. I. Ermakov[a], I. V. Yurova[a], A. D. Davydov[b], B. A. Khorishko[a], A. P. Lar'kov[c], and K. V. Stanislavchik[d]

[a] *Novomoskovsk Institute at D.I. Mendeleev University of Chemical Technology of Russia, ul. Druzhby 8, Novomoskovsk, 301650 Russia*
e-mail: AErmakov@dialog.nirhtu.ru

[b] *A.N. Frumkin Institute of Physical Chemistry and Electrochemistry of Russian Academy of Sciences, Moscow, Russia*

[c] *OOO "Kortekor Grupp," Novomoskovsk, Russia*

[d] *OAO "Rossiiskaya Elektronika," Moscow, Russia*

Received July 16, 2012

Abstract—Geometry and electronic structure of magnetite minimal cluster $(Fe_3O_4)_1$ have been simulated by density functional theory and semiempirical PM6 method. Data on the cluster geometry obtained by different methods have been consistent; however, the ground state electronic structures as determined by different methods have not been identical. The existence of two states of similar stability, low-spin and high-spin ones, has been predicted. The correlation of the simulated geometry, vibration spectra, and magnetic properties of the cluster with experimentally determined properties of magnetite, nanomagnetite, and magnetite thin films has been discussed.

DOI: 10.1134/S1070363213080033

Magnetite Fe_3O_4 is highly thermodynamically stable and is widely applied as magnetic material, catalyst, and sorbent; it affects the biological processes in living organisms and is important for medical applications. In the process of steel corrosion, magnetite is known to form passivating films. Magnetite is applied as a material of anticorrosion coatings and "sacrificial" anodes. The $(Fe_3O_4)_n$ clusters may serve as components of new materials based on nanostructured magnetite, and thus are of interest for electrical engineering, electronics, electrochemistry, and in other fields. They are also relevant models of reactive sites of magnetite surface in chemical and electrochemical processes. The geometry and electronic structure of clusters formed by iron and oxygen have been intensively studied by both experimental and theoretical methods [1–3]. However, clusters corresponding to the magnetite stoichiometry $(Fe_3O_4)_n$ have not yet been systematically studied. Some properties of the simplest cluster (n = 1) have been presented and discussed [4–7], it should be noted that the data available on its geometry, stability, and the ground state spin multiplicity are somewhat contradictory. Inspired by the above-discussed reasons, we determined in this work the structure and some properties of this cluster by means of quantum-chemical calculations, and discussed it in more detail.

The spatial structure, total energies, Gibbs energies of formation from atoms and minimal substances, vibration spectra, and magnetic moments in the ground electronic states of the $(Fe_3O_4)_1$ cluster were obtained. This cluster had an even number of electrons, thus, its states at different spin multiplicities were considered ($M = 2S + 1$, with S being sum of spin quantum number over all electrons): 1, 3, 5, 7, 9, 11, 13, 15, and 17. The calculations were performed with geometry optimization at different multiplicities by means of the density functional theory DFT under the following approximations: B3LYP/6-31G*, PBE/6-31G*, and PW91/6-31G* (Firefly quantum-chemical software package) [8]; PBE/3z, PBE/4z, and PBE/sbk (PRIRODA) [9–11]. The selected all-electronic basis sets (6-31G* [12, 13], 3z, and 4z [10]) were significantly different in the breadth. By using the electron endowment with the basis set functions in the cluster [14] as a parameter, it could be estimated that in the series of the selected sets the breadth increased 2.7 times: 6-31G* (0.941) < 3z (1.293) << 4z (2.510). It is noteworthy that as the basis set breadth increased,

its disbalance with respect to the endowment parameter also increased. In the 6-31G* basis set each iron electron was provided with the basis functions 0.876 times that of the oxygen electrons. In the 3z and 4z basis sets this ratio was even less (0.678 and 0.651, respectively). Thus, it was reasonable to compare the results obtained using different basis sets.

The quantum-chemical simulation of the $(Fe_3O_4)_1$ cluster structure by means of Hartree-Fock method with the wavefunctions both restricted by spin (RHF and ROHF) and non-restricted (UHF), as well as by DFT in the ROHF approximation failed: the self-consistency procedure did not converge at the stage of energy determination at the fixed geometry. Only DFT simulation under the RHF (M = 1) and UHF (M = 3, 5, 7, 9, 11, 13, 15, and 17) approximations in most cases gave the self-consistent solution.

The DFT simulation quality was checked in [23] in the case of FeO cluster using the BPW91, BLYP, and B3LYP exchange-correlation functionals with the 6-311+G* basis set. The exchange-correlation functional applicability in description of the bond length, dissociation energy, harmonic vibrational frequencies, dipole moment, and electron affinity were discussed. The effective charges and spin densities (magnetic moments) were presented. It was concluded that the B3LYP functional was the best to describe the bond length, dissociation energy, and electron affinity of FeO molecule.

Other studies of geometry, energy parameters, oscillation frequencies, magnetic moments, and other characteristics of iron oxide clusters of different stoichiometry by means of DFT were published in [1–5].

In this work the following functionals were applied: pure non-empirical exchange-correlation functional PBE [15], consecutively constructed and convenient for calculation acceleration [10]; pure functional PW91 [16, 17], widely used in the iron oxides clusters simulation [3, 4]; and hybrid B3LYP [18], suitable for the thermochemical properties description. As further larger molecular systems containing magnetite clusters will have to be simulated in future studies, we conducted the comparative simulation of the $(Fe_3O_4)_1$ cluster by faster methods, under the valence electrons approximation. The first method used was the approximation of the effective cire potential with the sbk pseudopotential (PRIRODA). The second method was the semiempirical quantum-chemical method, PM6 (standard parameterization in Mopac-2009 software [19, 20]). Calculation results were analyzed in the graphical packages ChemCraft [21] and Gabedit [22].

It should be noted that the spin states arrangement according to their energies was problematic in DFT methods, even though in some cases correct solutions were obtained [23–25]. Evidently due to complicated procedure of eliminating spin contamination from the wavefunction it was not discussed even in the case of the diatomic FeO molecule [23].

In our B3LYP/6-31G* simulations (UHF method), the spin contamination in the ground state wavefunction of the Fe_3O_4 cluster was dependent on the multiplicity as follows (M, contamination in %): 1, 0; 3, 147; 5, 79; 7, 10; 9, 4; 11, 2; 13, 0.18; 15, 0.09; 17, 0.05. Near the total energy minimum, that is, in the stable state, at M = 15 the spin contamination was negligible (0.09%). Note that even for organic compounds the spin contamination of less than 10% is usually neglected. Only for two cluster states in this work the spin contamination was high; due to this reason the energetically less stable state at M = 3 will not be discussed.

In attempt to eliminate the spin contamination completely, the $(Fe_3O_4)_1$ cluster was simulated by means of ROHF method, however, in all the trials the self-consistency procedure did not converge. All the attempts failed to get the self-consistent solution by altering the starting Hamiltonian and starting geometry, by introduction of positive charge, and by basis set reduction to a minimum one. This result might indicate that the spin-restricted wavefunction was not enough flexible and thus was a poor approximation for simulation of the systems like magnetite clusters, where the exchange interactions were important.

The magnetic properties of the cluster were discussed in this work with showing the full magnetic spin moment S, calculated as $2[S(S + 1)]^{1/2}$, in Bohr magnetons μ_B [26].

Energy parameters. Total energies of the $(Fe_3O_4)_1$ cluster as a function of electronic state spin multiplicity (relative to the most stable state energy) $\Delta_r E_{tot}$ are given in Table 1. These energies at the optimized geometry parameters and varied spin multiplicity were dependent on the exchange-correlation potential type and, to a lesser extent, on the basis set type.

Table 1. Calculated total energies $\Delta_r E_{tot}$ of the $(Fe_3O_4)_1$ cluster for different multiplicities (M) of the electronic state, kJ mol^{-1}[a]

M	B3LYP/6-31G*	PBE/6-31G*	PW91/6-31G*	PBE/3z	PBE/4z	PBE/sbk	PM6
1	344	187	–	204	195	312	152
3	292	–	–	8	24	–	92
5	0	–	–	0	0	0	62
7	194	–	–	11	86	31	0
9	141	–	–	50	61	–	36
11	94	19	–	46	33	70	103
13	45	0	0	17	15	27	151
15	8	20	23	29	29	11	436
17	182	236	241	253	255	213	570

[a] The dash indicates that stationary point of the stable state was not found.

From Fig. 1 it is seen that two total energy minima were obtained by DFT method. The first minimum corresponded to the low-spin state of the cluster at M = 5 or 7. The total spin magnetic moment of the cluster was equal to 4.90 and 6.94 μ_B, respectively, unlike the result obtained by means of molecular dynamics with the PW91 functional under pseudopotential approximation and in the planewaves basis (4.00 μ_B) [4]. The second minimum, only 8–17 kJ mol^{-1} higher in the energy (Table 1), corresponded to the high-spin state of the cluster at M = 13 or 15. In the latter case, the spin magnetic moment of the cluster equaled 12.98 and 14.98 μ_B, respectively.

The basis set extension in the 6-31G*–3z–4z row, the exchange-correlation functional being the same (PBE), did not influence the result significantly. The multiplicities of the first and the second minima of energy remained the same. Results of simulation in the sbk basis were in line with the data of calculation in all-electron basis, especially close to the multiplicities corresponding to the two local minima. The semiempirical PM6 method pointed at a single energy minimum at M = 7, and gave the cluster energies $\Delta_r E_{tot}$ close to the mean of simulation results by PW91/6-31G* and PBE/4z (Table 1) in the M range of 1–11.

The corresponding Gibbs energies $\Delta_r G^0_{298}$ changed in line with the total energies (Table 2); thus, the total energy was a suitable parameter to estimate the clusters stability. The negative Gibbs energies of the cluster formation from atoms and from minimal substances were indications of thermodynamic stability of the isolated $(Fe_3O_4)_1$ cluster.

From Table 2 data it also followed that the PBE/4z and PBE/sbk methods predicted the higher stability of the cluster than did the B3LYP/6-31G* method. The experimental thermodynamic functions have not been available so far for the $(Fe_3O_4)_1$ cluster, so let us consider other data. From results of [23] it followed that the dissociation energy of FeO molecule was calculated the best in the 6-311G* basis set using the B3LYP exchange-correlation functional, the relative calculation error ε was ~3%. The BLYP and BPW91 functionals gave much higher errors, ~25 and ~27%, respectively. Our calculations of the standard enthalpy of formation for FeO from minimal substances ($\Delta_f H^0_{298}$) also led to the conclusion of B3LYP superiority. Indeed, at the optimized value of M = 5, the values of $\Delta_f H^0_{298}$, kJ mol^{-1} (ε, %) for the B3LYP/6-31G*, PBE/6-31G*, PW91/6-31G*, PBE/3z, PBE/4z, and PBE/sbk methods were: 277 (8.5), 124 (51.6), 98 (61.6), 118 (53.6), 135 (47.3), and 131 (48.8), respectively. The $\Delta_f H^0_{298}$ calculation error in the case of the B3LYP/-31G* method was comparable to that of the PM6 method [$\Delta_f H^0_{298}$ and ε were 276 (8.1) at M = 3 and 290 (13.3) at M = 5], experimental $\Delta_f H^0_{298}$ being 255.6 kJ mol^{-1} [27].

Basing on the above-mentioned results, it was reasonable to estimate the $(Fe_3O_4)_1$ cluster enthalpy of formation from the minimal substances as the result of B3LYP/6-31G* calculation: –345 (M = 5) and –337 (M = 15), or –340 kJ mol^{-1} on the average.

Spatial structure. The $(Fe_3O_4)_1$ cluster geometry was first suggested in [28]. That structure was confirmed by simulations. Depending on the multiplicity,

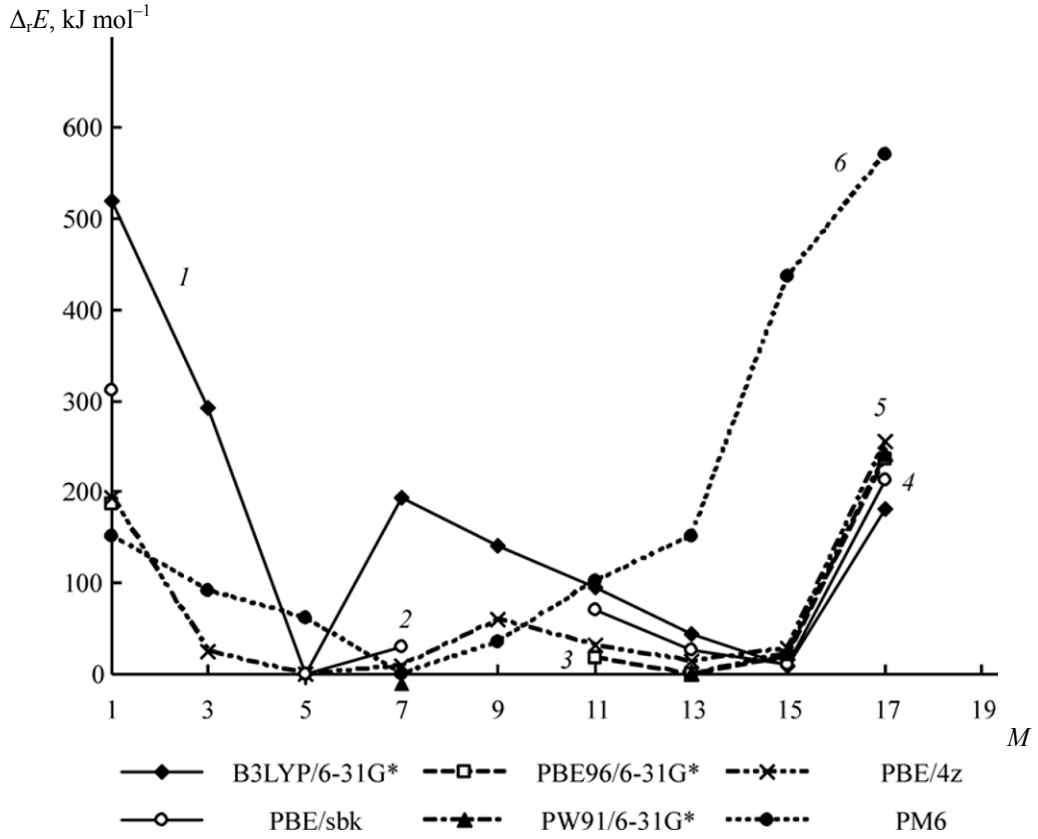

Fig. 1. Calculated total energy $\Delta_r E_{tot}$ of the $(Fe_3O_4)_1$ cluster atoms as a function of the spin multiplicity of the electronic state.

9 Fe–O and 3 Fe–Fe bonds might exist in the cluster. The cluster geometry was of a distorted pyramid, the bond lengths being slightly changed with multiplicity variation. The pyramid base was formed by the iron atoms connected via the equatorial oxygen atoms (O_e). In the pyramid vertex the oxygen axial atom (O_a) was located forming the bonds with the iron atoms of the base (Fig. 2). All DFT calculations, independent of the

Table 2. Calculated Gibbs energies of the $(Fe_3O_4)_1$ cluster for different multiplicities (M) of the electronic state: relative ($\Delta_r G^0_{298}$), of formation from the isolated atoms ($\Delta_a G^0_{298}$), and of formation from minimal compounds ($\Delta_f G^0_{298}$), kJ mol^{-1}[a]

M	B3LYP/6-31G*			PBE/4z			PBE/sbk		
	$\Delta_r G^0_{298}$	$-\Delta_a G^0_{298}$	$-\Delta_f G^0_{298}$	$\Delta_r G^0_{298}$	$-\Delta_a G^0_{298}$	$-\Delta_f G^0_{298}$	$\Delta_r G^0_{298}$	$-\Delta_a G^0_{298}$	$-\Delta_f G^0_{298}$
1	530	1869	–174	208	2368	325	323	2286	243
3	293	2106	63	25	2551	508	–	–	–
5	0	2399	356	0	2576	533	0	2609	566
7	193	2206	163	90	2486	443	31	2578	535
9	142	2257	214	60	2516	473	–	–	–
11	93	2306	263	35	2540	498	71	2538	495
13	41	2358	315	18	2558	515	29	2580	537
15	10	2389	346	32	2544	501	15	2594	551
17	177	2222	179	257	2319	276	214	2395	352

[a] The reference Gibbs energy of the isolated atoms formation from the minimal compounds (371.3 and 231.8 kJ mol^{-1} for iron and oxygen, respectively) [27] were used in $\Delta_f G^0_{298}$ calculations.

ground states multiplicity, gave approximately the same structure. The PM3 semiempirical method predicted somewhat shorter Fe–O_a bonds (Table 3).

In the magnetite crystal lattice, there were 4 Fe–O bonds of 187.6 pm length (tetragonal coordination of iron) and 6 bonds of 206.6 pm length (octahedral coordination of iron) [29]. From Fig. 3 it is seen that the calculated lengths of Fe–O_e bond were somewhat smaller than the Fe–O distance of the tetrahedrally coordinated magnetite iron atoms. This was expected, as the Fe–O_e bond angles in the cluster were close to the tetrahedral ones. For example, according to the B3LYP/6-31G* data, at M = 15 the O_eFeO_e bond angles were in the range of 129–138°. The Fe–O_a bonds were longer than Fe–O_e bonds. However, they were shorter than the interatomic distances Fe–O in the magnetite crystal lattice at the octahedral coordination of iron. The Fe–O_a lengths were intermediate between the Fe–O lengths in the cases of octahedral and tetrahedral coordination of iron in magnetite.

The interatomic Fe–Fe distances in the cluster (Fig. 3) were by ~20% smaller than the shortest Fe–Fe distance in magnetite (297 pm). It is known that the relaxation of (001) magnetite surface covered with the tetrahedral iron atoms layer is accompanied by the compression of the distance between the first two layers by up to 40% as compared to that in the crystal bulk [31]. Thus, the $(Fe_3O_4)_1$ cluster may be considered a model of the magnetite surface fragment.

The calculated Fe–Fe distance (Table 3) was close to the Fe–Fe bond length in the tris(iron) complexes (~246 pm [30]), for example, in $Fe_3(CO)_9$. It was also close to the interatomic distance in the isolated Fe_3 cluster. Recently, its structure has been determined: C_{2v} with the Fe–Fe bond length of 207 and 238 pm [32], even though reference data on Fe_3 structure and ground state are contradictory.

Our simulation of Fe_3 cluster by B3LYP/6-31G* and PBE/3z methods also revealed that the average Fe–Fe distance in the metal cluster was somewhat smaller than that in the minimal magnetite cluster. Indeed, r(Fe–Fe) was 229 pm in the case of Fe_3 (optimized M = 9) and 248 pm in the case of $(Fe_3O_4)_1$ (M = 5) with B3LYP/6-31G* or 226 pm (M = 11) and 249 pm (M = 5) with BPE/3z. This pointed at some weakening of the Fe–Fe bond in $(Fe_3O_4)_1$ as compared with Fe_3, even though the symmetry of the iron atoms arrangement was preserved. This result allowed estimating the Fe–O bond energy of the studied

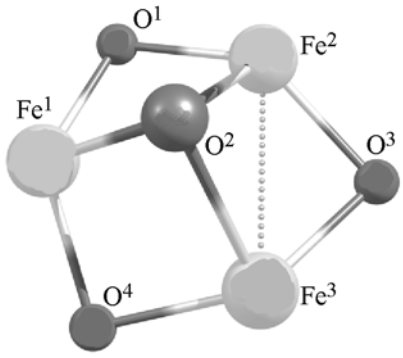

Fig. 2. Spatial structure of the $(Fe_3O_4)_1$ cluster.

cluster. According to our data (B3LYP/6-31G*), the binding energy of the Fe_3 cluster equaled –138 kJ mol^{-1}, thus the expected total Fe–O energy of the most stable $(Fe_3O_4)_1$ cluster (at M = 15) was about –2260 kJ mol^{-1}. Then, the average energy per each of 9 Fe–O bonds in the cluster was ~250 kJ mol^{-1}. Thus, Fe–O bonds were important in the cluster stabilization, in line with the data of [3] on the role of such bonds in the iron oxides clusters with up to 5 iron atoms.

Vibration spectrum. IR spectrum of magnetite nanoparticles contained a band of medium intensity at 440 cm^{-1} and a very intensive broad band at 590 cm^{-1}. The low-frequency band was assigned to the Fe–O in the octahedral lattice point vibrations, and the high-frequency band was due to vibrations of the tetrahedral lattice point [33]. The cluster vibration spectrum simulated by different methods is presented in Table 4.

The simulated IR spectrum of the $(Fe_3O_4)_1$ cluster contained bands of medium intensity corresponding to the Fe–O_e bonds vibrations in the range of experimental low-frequency band. The high-frequency experimental band range of the simulated spectrum contained the intensive bands as well; the corresponding vibrations were those of Fe–O_a bonds. The cluster spectrum simulated by means of B3LYP/6-31G* at M = 5 and 15 was the most consistent with the nanomagnetite experimental spectrum.

Magnetic properties. The bulk magnetite sample is a ferrimagnetic material, and the magnetic moment per formula unit is of 4 μ_B. However, the magnetic moment per formula unit of magnetite thin film was much higher [34, 35]. Recalculation of the experimental data showed that at the film thickness comparable to the characteristic size of the $(Fe_3O_4)_1$ cluster (0.35 nm), the magnetic moment was 13.6 [34] and 17.4 μ_B [35] per formula unit. Those values were close to 14.97 μ_B, the magnetic moment of the high-spin

Table 3. Calculated internuclear distances for the $(Fe_3O_4)_1$ cluster, pm

Bond	B3LYP/6-31G*		PBE/6-31G* (*M* 13)	PW91/6-31G* (*M* 13)	PBE/3z (*M* 5)	PBE/4z (*M* 5)	PBE/sbk (*M* 5)	PM6 (*M* 7)
	M 5	*M* 15						
Fe–O_e equatorial bonds								
Fe^1–O^1	182	182	183	183	181	181	182	171
O^1–Fe^2	182	182	183	182	182	182	182	191
Fe^2–O^3	183	184	183	183	182	182	182	181
O^3–Fe^3	180	181	180	179	181	181	182	181
Fe^3–O^4	179	181	180	179	185	184	184	191
O^4–Fe^1	183	184	183	183	185	184	184	171
Fe–O_a axial bonds								
Fe^1–O^2	198	198	202	202	202	202	202	186
Fe^2–O^2	198	198	203	203	191	191	191	184
Fe^3–O^2	191	195	179	179	202	201	202	184
Fe–Fe bonds								
Fe^1–Fe^2	254	251	257	257	252	250	254	253
Fe^2–Fe^3	236	240	228	228	252	350	254	252
Fe^1–Fe^3	254	251	228	228	243	241	242	253

state (M = 15) of the $(Fe_3O_4)_1$ cluster. The exclusively high magnetic moment of the epitaxial magnetite films was likely due to the formation of $(Fe_3O_4)_1$-like structures at the phase boundaries.

Electrons distribution. The effective Hirshfeld atom charges (Q) of the $(Fe_3O_4)_1$ cluster computed by PBE/4z method are shown in Fig. 4 as a function of the spin multiplicity.

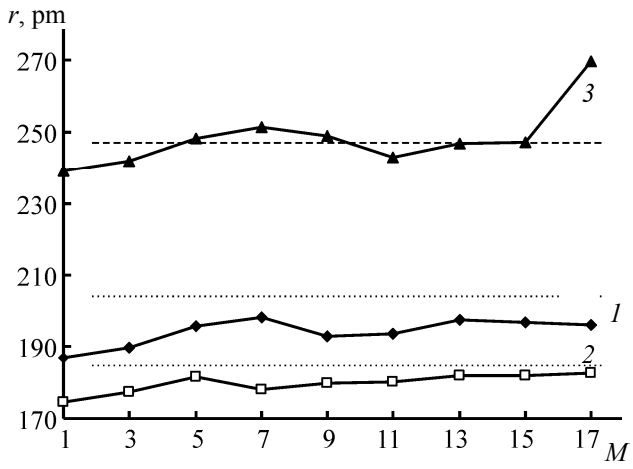

Fig. 3. Mean bond lengths in the $(Fe_3O_4)_1$ cluster atoms as a function of the multiplicity of the electronic state, as calculated by B3LYP/6-31G* method: (*1*) Fe–O_a; (*2*) Fe–O_e; and (*3*) Fe–Fe. (The dotted lines) indicate the Fe–O bond length in magnetite [29], (the dashed line) shows the Fe–Fe bond length in tris(iron) complex [30].

In the singlet state, the Q value for all the oxygen atoms was the same, –0.22 a. u. Two of iron atoms bear the charge of 0.33 a. u., while the third one had the charge of 0.24 a. u. Such distribution corresponded to the classical scheme of magnetite structure: iron(II) ferrate(III). As M increased, the effective charges change was nonmonotonous, but the pair of iron atoms with the higher charge, the charge of the third iron atom being lower, was preserved up to M = 13, inclusively. In the high-spin cluster states (M = 15 and 17) the effective charges of all three iron atoms were the same. Equatorial oxygen atoms also had the same negative charge, while the axial oxygen atom in all the open-shell states had smaller negative charge.

The spin density distribution (P^α) of the iron atoms at M = 3, 5, 7, 9, 11, and 13 (Fig. 5) reflected the ferrimagnetic properties of magnetite.

One of the iron atoms was characterized by smaller value of P^α than the other two. At M = 15 and 17 all iron atoms of the cluster had the same value of P^α, which pointed at paramagnetism. The P^α values of oxygen atoms increased from –0.05 to 0.74 a. u. at increasing M.

Table 4. Calculated IR spectrum of the $(Fe_3O_4)_1$[a] cluster (wavenumbers of the normal vibrations, ν, cm^{-1})

B3LYP/6-31G*		PBE/6-31G* (*M* 13)	PW91/6-31G* (*M* 13)	PBE/3z (*M* 5)	PBE/4z (*M* 5)	PBE/sbk (*M* 5)	PM6 (*M* 7)	Experiment[b]
M 5	*M* 15							
143	65	*160*	*161*	*84*	*83*	*105*	165	
178	127	170	170	149	149	152	*172*	
222	228	224	224	160	*156*	171	*324*	
223	250	256	256	188	189	196	340	
249	263	259	260	222	221	228	*361*	
322	334	*301*	*302*	*271*	*271*	282	**397**	
335	*355*	334	335	*278*	*277*	286	*440*	
386	*377*	371	369	*313*	*315*	322	**516**	
434	464	444	447	436	435	446	*520*	440
507	*487*	459	462	472	468	485	548	
571	**569**	**534**	**537**	**488**	**486**	**509**	601	
611	**582**	**660**	**661**	**528**	**528**	**537**	626	**590**
688	694	680	682	620	622	625	*750*	
704	**733**	**720**	**722**	**637**	**638**	**641**	**768**	
745	**745**	**735**	**738**	**670**	**670**	**674**	**807**	

[a] Data are shown for the most stable cluster states, wavenumbers for the transitions of low intensity are shown in italic, those of medium intensity are shown in regular font, those of high intensity are shown in bold. [b] Experimental data for nanomagnetite [30].

According to calculations by the density func-tional method, two states of similar energy, the low-spin and the high-spin, corresponded to the minimal magnetite cluster $(Fe_3O_4)_1$. The Fe–O and Fe–Fe bonds length in the cluster were smaller than those in bulk magnetite. The average Fe–O energy estimate was ~250 kJ mol^{-1}, the standard enthalpy of formation from the minimal substances was –340 kJ mol^{-1}. The normal vibrations frequencies of the cluster atoms corresponded to the characteristic frequencies of nanomagnetite. The sharp increase of magnetization with decrease of the thickness of epitaxial thin magnetite films might be

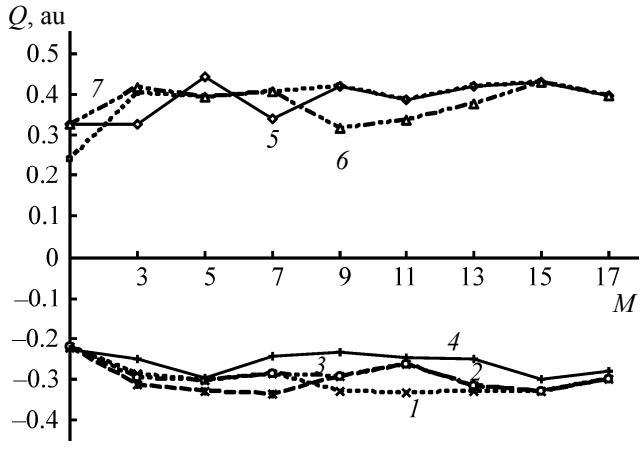

Fig. 4. Effective charges at the $(Fe_3O_4)_1$ cluster atoms as a function of the multiplicity of the electronic state, as calculated by PBE/4z method: (*1*, *2*, *3*) equatorial oxygen atoms; (*4*) axial oxygen atom; (*5*, *6*, *7*) iron atoms.

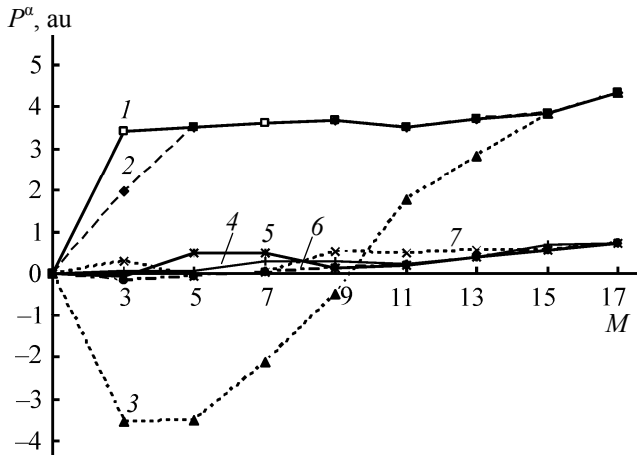

Fig. 5. Spin electron density of the $(Fe_3O_4)_1$ cluster atoms as a function of the multiplicity of the electronic state, as calculated by PBE/4z method: (*1*, *2*, *3*) iron atoms; (*4*, *5*, *6* *7*) oxygen atoms.

due to the appearance of the high-spin state of the $(Fe_3O_4)_1$ cluster.

REFERENCES

1. Palotás, K. and Andriotis, A.N., *Phys. Rev. B.*, 2010, vol. 81, p. 075403-1.
2. Roy, D.R., Robles, R., and Khanna, S.N., *J. Chem. Phys.*, 2010, vol. 132, p. 194305-1.
3. Xu, B.-F., Yang, C.-L., Wang, M.-S., and Ma, X.-G., *J. Mol. Struct. (Theochem.)*, 2010, vol, 957, nos. 1–3, p. 26.
4. Shiroishi, H., Oda, T., Hamada, A.I., and Fujima, A.N., *Eur. Phys. J. D.*, 2003, vol. 24, p. 85.
5. Reddy, B.V., Rasouli, F., Hajaligol, M.R., and Khanna, S.N., *Fuel*, 2004, vol. 83, nos. 11–12, p. 1537.
6. Yurova, I.V., Ermakov, A.I., Khorishko, B.A., and Ivanova, O.V., *Proc. Univ. Ser. Chem. Chem. Technol.*, 2008, vol. 51, no. 5, p. 37.
7. Khorishko, B.A., Ermakov, A.I., Davydov, A.D., Ivanova, O.V., and Yurova, I.V., *Rus. J. Electrochem.*, 2009, vol. 45, no. 8, pp. 941–945.
8. Granovsky, A.A., Firefly ver. 7.1.G; *http://classic.-chem.msu.su/gran/firefly/index.html*.
9. Laikov, D.N.. *Chem. Phys. Lett.*, 1997, vol. 281, p. 151.
10. Laikov, D.N., *Candidate Sci. (Chem.) Dissertation*, Moscow, 2000.
11. Laikov, D.N. and Ustynyuk, Yu.A., *Rus. Chem. Bull.*, 2005, vol. 54, no. 3, pp. 820–826.
12. Hehre, W.J., Ditchfield, R., and Pople, J.A., *J. Chem. Phys.*, 1972, vol. 56, p. 2257.
13. Rassolov, V.A., Pople, J.A., Ratner, M.A., and Windus, T.L., *J. Chem. Phys.*, 1998, vol. 109, p. 1223.
14. Ermakov, A.I. and Yurova, I.V., *Rus. J. Phys. Chem. A*, 2010, vol. 84 , no. 11, pp. 1921–1929.
15. Perdew, J.P., Burke, K., and Ernzerhof, M., *Phys. Rev. Lett.*, 1996, vol. 77, p. 3865.
16. Perdew, J.P., Chevary, J.A., Vosko, S.H., Jacson, K.A., Pederson, M.R., Singh, D.J., and Fiolhais, C., *Phys. Rev., B,* 1992, vol. 46, p. 6671.
17. Perdew, J.P., *Physica*, *B,* 1991, vol. 172, p. 1.
18. Becke, A.D., *J. Chem. Phys.*, 1993, vol. 98, p. 5648.
19. Stewart J.J.P., *MOPAC2009; http://OpenMOPAC.net. 2009*.
20. Stewart, J.J.P., *J. Mol. Modeling,* 2007, vol. 13, p. 1173.
21. Zhurko, G.A., and Zhurko, D.A., *Chemcraft, ver. 1.6. build 348; www.chemcraftprog.com*.
22. Allouche, A.R., *J. Comput. Chem.,* 2011, vol. 32, p. 174.
23. Gutsev, G.L., Rao, B.K., and Jena, P., *J. Phys. Chem. (A),* 2000, vol. 104, no 22, p. 5374.
24. Zhao, Y. and Truhlar, D.G., *J. Chem. Phys.*, 2006, vol. 124, no 22, p. 224105-1.
25. Sorkin, A., Iron, M.A., and Truhlar, D.J., *J. Chem. Theory Comput.*, 2008, no. 4, p. 307.
26. Kalinnikov, V.T. and Rakitin, Yu.V., *Vvedenie v magnetokhimiyu. Metod staticheskoi vospriimchivosti v khimii.* (Introduction to Magnetochemistry. Method of Static Magnetic Susceptibility in Chemistry), Moscow: Nauka, 1980.
27. Belov, G.V., Iorish, V.S., and Yungman, V.S., *High Temp*., 2000, vol. 38, no. 2, pp. 191–196.
28. Wang, L.-S., Wu, H., and Desai, S.R., *Phys. Rev. Lett.,* 1996, vol. 76, no. 25, p. 4853.
29. Antonov, V.N., Bekenov, L.V., and Yaresko, A.N., *Adv. Condens. Matt. Phys.*, 2011.
30. Pauling, L., *Proc. Natl. Acad. Sci. USA.*, 1976, vol. 73, no. 12, p. 4290.
31. Mijiritskii, A.V. and Boerma, D.O., *Surf. Sci.*, 2001, vol. 486, p. 73.
32. Samah, M., and Moula, B., *Revista Mexicana de fisica*, 2011, vol. 57, no. 2, p. 166.
33. Dikii, N.P., Dobbnya, A.N., Medvedeva, E.P., Khlapova, N.P., Fedorec, I.D., Uvarov, V.L., Lyashko, Yu.V., *Proc. Kharkov Univ.*, 2008, vol. 823, no. 3, p. 78.
34. Wu, H.C., *A Thesis for the Degree of Doctor of Philosophy*, Dublin: School of Physics, Trinity College, 2009.
35. Orna, J., Morellón, L., Algarabel, P.A., de Teresa, J.M., Fernández-Pacheco, A., Simón, G., Maden, C., Pardo, J.A., and Ibarra, M.R., *Adv. Sci. Technol.*, 2010, vol. 67, p. 82.